Experimental modal analysis technique for three-dimensional acoustic cavities

Chaw-Hua Kung[a] and Rajendra Singh
Department of Mechanical Engineering, The Ohio State University, 206 West 18th Avenue, Columbus, Ohio 43210

(Received 3 February 1984; accepted for publication 27 August 1984)

This paper substantially advances Nieter and Singh's acoustic modal analysis technique [J. Acoust. Soc. Am. 72, 319–326 (1983)] which used the coincident-quadrature response method to extract acoustic global properties of one-dimensional systems. Here a technique to identify modal parameters including damping of a three-dimensional cavity is proposed. The cavity is excited by a convertible acoustic driver whose volume velocity is monitored. Acoustic transfer impedance database is obtained for a number of cavity boundary locations which are chosen such that all modes of interest can be adequately described. The vector diagram method is used to fit the measured database in the neighborhood of each resonance frequency with a circle. The experimental technique proposed here has been verified by applying it first to a cylindrical cavity whose exact eigensolutions are known. Then for an annularlike cavity, experimentally extracted natural frequencies and pressure mode shapes are found to agree well with the results of a finite element model. The significance of this paper lies in the successful demonstration of an experimental technique which can be used for diagnosing the acoustics of irregular shaped cavities. The proposed technique also offers an alternative to the finite element method for acoustic modal analysis of three-dimensional ducts and resonators of irregular shapes and/or with complicated boundary conditions.

PACS numbers: 43.85.Bh, 43.20.Ks, 43.85.Kr, 43.20.Bi

LIST OF SYMBOLS

b_i	pole for the ith mode
c	speed of sound (m/s)
f	frequency (Hz)
$f(i,m,n)$	natural frequency (Hz) corresponding to modal indices i (longitudinal z), m (circumferential θ), and n (radial r)
$[H]$	transfer function matrix
H_{kl}	element of $[H]$ in the k th row and the l th column
j	$\sqrt{-1}$
k_r, k_θ, k_z	wavenumbers in r, θ, and z directions, respectively
$\{N(\mathbf{r})\}$	shape function vector
p	acoustic pressure (Pa)
$\mathbf{r}$	position vector
$(r_{kl})_i$	residue of the ith mode corresponding to the response at k due to excitation at l
s	Laplace variable
t	time
U	volume velocity or flow rate (m^3/s)
z	specific acoustic impedance (Pa·s/m)
Z	acoustic impedance ($Pa·s/m^3$)
δ	Dirac delta function
ζ_i	damping ratio for the ith mode
ρ	density of the medium (kg/m^3)
$\psi_{(i,m,n)}$	pressure mode shape corresponding to modal indices i, m, and n
${}_k\psi_i$	k th component of the ith complex eigenvector
ω	circular frequency (rad/s)
ω_i	natural frequency for the ith mode (rad/s)
ω_{di}	damped natural frequency for the ith mode (rad/s)
∇^2	Laplace operator
$\{\nabla\}$	$\left(\frac{\partial}{\partial x}\frac{\partial}{\partial y}\frac{\partial}{\partial z}\right)^T$

Superscripts

$\cdot$	time derivative
$*$	complex conjugate
T	transpose

INTRODUCTION

Three-dimensional acoustic cavities are found in many engineering, architectural, and musical applications; typical

[a] Now at Department of Mechanical Engineering, Howard University, Washington, DC 20059.

 0001-4966/85/020731-08$00.80

examples include living rooms, automobile passenger compartments, and fluid spaces contained within machinery casing structures. Noise and vibration problems in some machines and engineering systems are often related to the acoustic oscillations in these cavities, which could be excited either aerodynamically or structurally.[1] Such objectionable oscillations can be reduced if suitable geometric changes are made such that acoustic resonances are avoided. Also, dissipative material liners or baffles can be placed in those regions where large acoustic amplitudes exist. However, the solution process requires that the cavity natural frequencies and modes be known. Since the cavities often encountered in practice are either geometrically irregular or possess complicated boundary conditions, computational or experimental methods must be adopted for the modal analysis.

The focus of this paper is on the experimental aspects with application to three-dimensional cylindrical or annularlike cavities. An experimental acoustic modal analysis technique is proposed here. Such a method could be very useful in not only investigating the acoustic behavior of irregular shaped ducts, cavities, and resonators but also could offer an alternative to the finite element method. The technique proposed here is validated by comparing measured results with those obtained analytically.

I. LITERATURE REVIEW

In the classical acoustic modal analysis experiment for three-dimensional cavities, the natural frequencies of an acoustic cavity were identified by exciting the cavity at a single frequency of interest and by observing the amplitude and phase (relative to a fixed or known signal) of the acoustic pressure response on an oscilloscope. This procedure was repeated at many discrete frequencies over the range of interest. The associated modes were identified from the pressure database acquired at various locations in the cavity. This technique employing pure sinusoidal excitation is obviously extremely time consuming and not very efficient. Petyt *et al.*'s[2] experiment for a rectangular cavity with incomplete partition is a typical example of such an experimental modal analysis technique.

With the advent of single channel frequency analyzers, natural frequencies could be directly identified from the frequency spectrum of the measured pressure data. Only a few spectra are required to find most of the resonance frequencies of interest. Au-Yang[3] has conducted such an experiment to find the natural frequencies of an annular cavity. The acoustic pressure mode shapes are still identified by measuring the relative acoustic pressure responses at various locations on the cavity boundary.

Since the early seventies and the advent of two channel FFT analyzers, identifying modal parameters from measured frequency response functions has increasingly been used for mechanical and structural systems. Klosterman[4] has provided a relationship between the measured dynamic compliance matrix and the complex eigenvalues and eigenvectors. Richardson[5] has given a detailed review of several modal analysis techniques using digital instrumentation systems. The theory and application of modal analysis techniques to structures are adequately covered in several publications.[6–8]

For a mechanical structure, the force and motion can be measured accurately using a force transducer and an accelerometer; therefore, reliable transfer functions are obtained without much difficulty. Conversely, for an acoustic system, only acoustic pressure can be measured directly with a microphone or a pressure transducer; thus the acoustic transfer functions such as the acoustic impedances or admittances can only be obtained through indirect means. Singh[9] has given a detailed review of acoustic impedance measurement techniques; most of which have been applied to one-dimensional acoustic systems. The acoustic modal analysis experiment, comparable to those techniques currently in practice for structures, was recently proposed by Nieter and Singh.[10] This technique has been validated by comparing experimental results of several one-dimensional ducts, over the plane-wave frequency regime, with theory.

II. OBJECTIVES

This paper is a logical extension of the earlier paper by Nieter and Singh[10] who used the coincident-quadrature response technique to extract acoustic global properties. We intend to concentrate here on the three-dimensional annularlike cavities whose modal properties including damping will be extracted using the vector diagram method. Our excitation method relies on the utilization of the convertible speaker method, as opposed to piston-shaker method employed by Nieter and Singh,[10] as we feel that this method is more suitable to three-dimensional acoustic systems. Unlike Nieter and Singh,[10] all pressure measurements are conducted at the boundary of the cavity. The scope of the problem is limited to a linear three-dimensional acoustic cavity with zero mean flow. Two example cases will be considered over the frequency range of about 0–2000 Hz for the air medium having room temperature (22.2 °C) at an ambient pressure. Appropriate review of conceptual and measurement considerations suitable for three-dimensional systems will be covered along with the demonstration of the proposed technique through two example cases.

III. CONCEPTUAL CONSIDERATIONS

With the assumptions of small perturbations, undamped system, zero mean flow, and negligible temperature gradient, the acoustic pressure response $p(\mathbf{r},t)$ of a three-dimensional acoustic cavity of volume V and boundary S excited by a point monopole located inside at $\mathbf{r}_s$ is governed by the following linear inhomogeneous wave equation

$$\nabla^2 p(\mathbf{r},t) - (1/c^2)\ddot{p}(\mathbf{r},t) = -\rho \dot{U}(t)\delta(\mathbf{r}-\mathbf{r}_s), \tag{1}$$

where c is the speed of sound, ρ is the medium density, $U(t)$ is the unsteady volume flow rate of the source, and δ is the Dirac delta function. Using the discrete system theory such as those used for finite element method formulations and introducing the energy dissipation term $[B]\{\dot{p}\}$, the behavior of the three-dimensional linear, damped acoustic cavity can be approximated by a set of second order linear differential equations of the form[12]

$$[A]\{\ddot{p}(t)\} + [B]\{\dot{p}\} + [C]\{p\} = \{q(t)\}, \tag{2a}$$

$$p(\mathbf{r},t) = \{N(\mathbf{r})\}^T\{p(t)\}, \tag{2b}$$

where $\{N(\mathbf{r})\}$ is the shape function vector, $\{q(t)\} = \lfloor 0 0 \cdots \dot{U}(t) \cdots 0 0 \rfloor^T$ is the acoustic forcing function (volume acceleration vector), $[A] = \int_V \{N\}\{N\}^T/(\rho c^2)dV$, $[B] = \int_s \{N\}\{N\}^T/Z\,dS$, z = specific acoustic impedance of the boundary, $[C] = \int_V \{N\}\{\nabla\}^T\{\nabla\}\{N\}^T/\rho\,dV$, and superscript T implies transpose. If the system has n degrees of freedom, the $[A]$, $[B]$, and $[C]$ are $(n\times n)$ and $\{p\}$ and $\{q\}$ are $(n\times 1)$. Taking the Laplace transform(s) of the system equations, assuming zero initial conditions and writing them in a transfer function form, we get

$$[s^2[A] + s[B] + [C]]\{p(s)\} = \{q(s)\}$$

or

$$\{p(s)\} = [H(s)]\{q(s)\}, \tag{3}$$

where $[H(s)]$ is the transfer function matrix $(n\times n)$. It has been shown that for an underdamped system, each element of $[H(s)]$ can be expressed as a partial fraction expansion of modal parameters

$$H_{kl}(s) = \sum_{i=1}^{n}\left(\frac{{}_k\psi_{il}\psi_i}{a_i(s-b_i)} + \frac{{}_k\psi_{il}^*\psi_i^*}{a_i^*(s-b_i^*)}\right), \tag{4}$$

where ${}_k\psi_i$ is the k th component of the ith complex eigenvector which satisfies $[H]^{-1}\{\psi\}_i = \{0\}$, a_i is the complex scaling for the ith mode, b_i is the pole for the ith mode $= -\zeta_i\omega_i + j\omega_i\sqrt{1-\zeta_i^2} \equiv -\zeta_i\omega_i + j\omega_{di}$, ζ_i is the damping ratio for the ith mode, ω_i is the natural frequency for the ith mode, and the superscripted asterisk denotes the complex conjugate. Frequency response function is obtained by replacing s with $j\omega$ in the above equation. Acoustic impedance Z is defined as

$$\begin{aligned} Z_{kl}(\omega) &= (p_k/U_l)(\omega) = j\omega H_{kl}(\omega) \\ &= \sum_{i=1}^{n}\left(\frac{j\omega\,{}_k\psi_{il}\psi_i}{a_i(j\omega-b_i)} + \frac{j\omega\,{}_k\psi_{il}^*\psi_i^*}{a_i^*(j\omega-b_i^*)}\right) \\ &= \sum_{i=1}^{n}\left(\frac{(r_{kl})_i}{j\omega-b_i} + \frac{(r_{kl})_i^*}{j\omega-b_i^*}\right), \end{aligned} \tag{5}$$

where $(r_{kl})_i$ is the residue of the ith mode. Note that the above expression for $Z_{kl}(\omega)$ is similar to that defined for a structure in terms of dynamic mobility. The contribution from each mode is determined by two complex variables, namely, its pole (b_i) and residue $((r_{kl})_i)$, thus there are $2n$ complex unknowns for the entire acoustic system of interest. Only one row or column of the transfer function matrix needs to be determined in order to solve all the unknowns provided no higher order (>2) pole exists.

The above considerations lead to an experimental technique to extract modal parameters (eigenvalues and eigenvectors) from measured acoustic impedances. Using the technique, a continuous acoustic cavity is approximated by a lumped-parameter model with finite number of measurement points. This model now yields the acoustic behavior of the cavity.

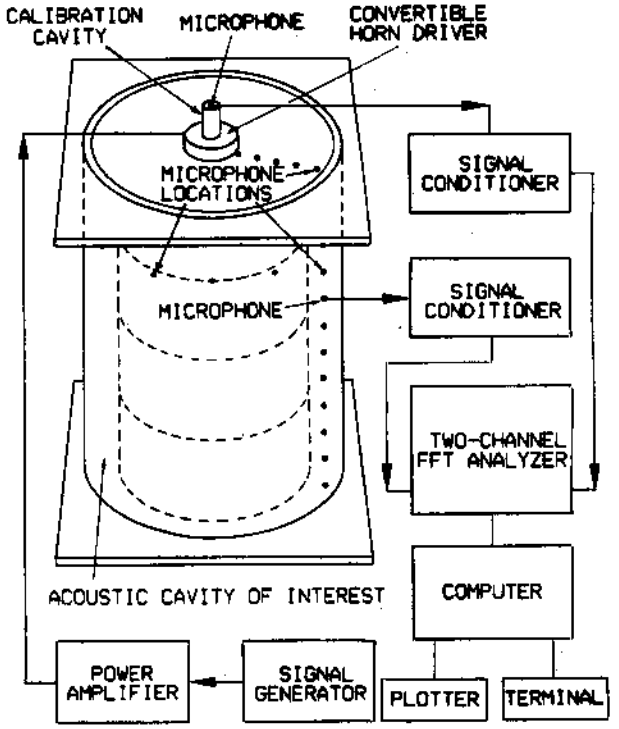

FIG. 1. Experimental setup and instrumentation.

IV. MEASUREMENT CONSIDERATIONS

A. Measurement of cavity impedances

Figure 1 shows schematically the arrangement of the experimental test setup and instrumentation. The acoustic cavity of interest is bounded by a closed cylindrical duct outside and by a circular cylinder inside. The cavity is excited by a convertible acoustic driver mounted either on the side of the cylindrical duct or on the top cover plate of the duct. The speaker location is chosen such that all modes of interest can be excited. The convertible driver technique, used earlier by Singh and Schary[11] for one-dimensional acoustic systems, has been extended here to three-dimensional cavities. A small enclosure of known volume is attached to the back of the driver for calibration purpose. Pressure responses are measured at 25 locations with a 3-mm microphone across the outer boundary. There are 6, 8, and 12 measurement stations along r, θ, and z directions, respectively. A transfer function diagram which relates the inputs of the system to outputs is shown in Fig. 2; here voltage fed to the convertible acoustic driver is $e(t)$, driving point acoustic impedance is Z_{ll} which relates the volume velocity $U_l(t)$ and the acoustic pressure $p_l(t)$ at the excitation point l of the

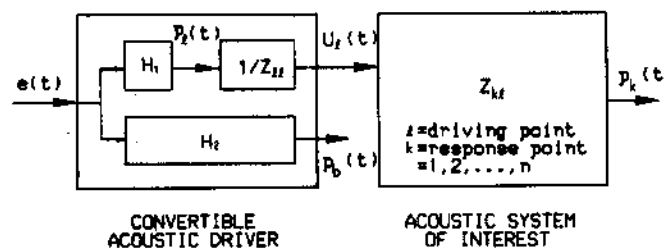

FIG. 2. Transfer function diagram of the acoustic driver and cavity of interest.

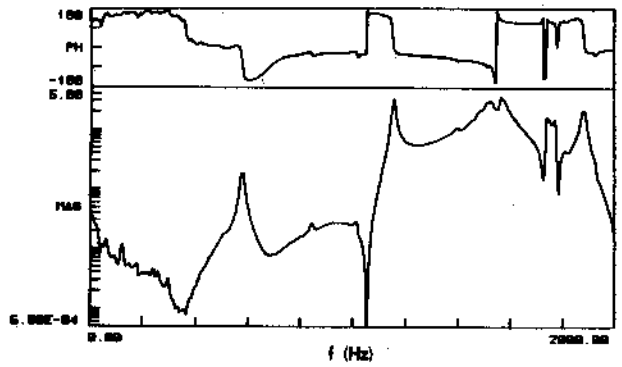

FIG. 3. Experimentally measured transfer function $p_k/p_b(\omega)$.

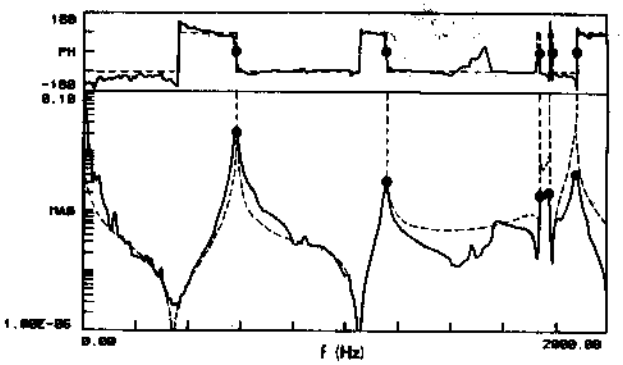

FIG. 5. Typical acoustic transfer impedance $p_k/U_l(\omega)$; — measured, ··· theory and ● —location of resonance.

acoustic system of interest, pressure in the calibration cavity of the driver is $p_b(t)$, pressure measured at k th response point is $p_k(t)$, and H_1 and H_2 are transfer functions related to the acoustic driver geometry and dynamics. With a two channel FFT analyzer, transfer functions are obtained by feeding bandlimited white noise to the acoustic driver and measuring two signals simultaneously. Figures 3 and 4 illustrate typical measured transfer functions $p_k/p_b(\omega) = Z_{kl}H_1/Z_{ll}H_2$ and $p_b/U_l(\omega) = H_2Z_{ll}/H_1$, and Fig. 5 shows their complex product Z_{kl} which is the transfer acoustic impedance of the cavity between locations k and l; it is also compared here with theoretical transfer impedance without damping. Fifty averages have been taken for each transfer function measurement to ensure good spectral estimations over 0–2000 Hz with bandwidth equal to 5 Hz. For the acoustic driver considered in this analysis, the transfer function H_1/Z_{ll} is fairly flat over the frequency range of interest. Thus Z_{kl} could be approximated by $p_k/e(\omega)$ if desired, which would be somewhat easier to measure.

B. Identification of modal parameters

A number of techniques are available for identifying modal parameters from the measured frequency response functions.[5] If natural frequencies are not closely spaced and modal damping ratios are very small, one can easily use co-

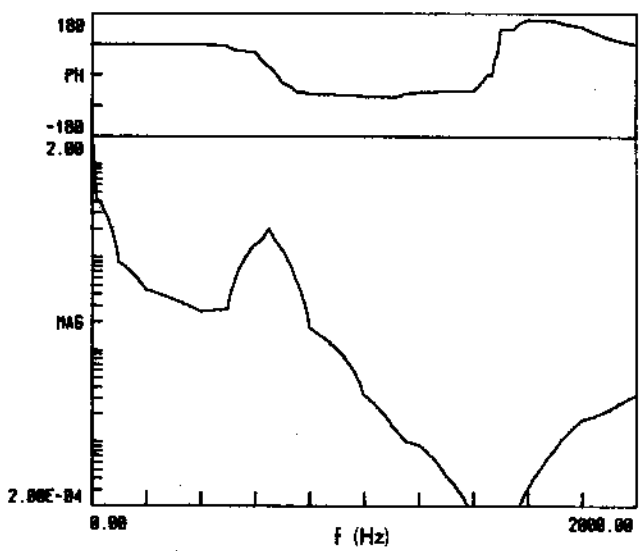

FIG. 4. Calibration transfer function p_b/U (ω).

quad (real–imaginary) plot technique as demonstrated by Nieter and Singh.[10] But if natural frequencies are close and the damping is moderate, then the vector diagram method, also known as Kennedy–Panku method, is more suitable. The frequency response is presented by plotting the real part (Re) versus the imaginary part (Im) at equal frequency increments as shown in Fig. 6.

The frequency response function for a single mode (l), from Eq. (5), is

$$H_l(j\omega) = [r_l/(j\omega - b_l)] + [r_l^*/(j\omega - b_l^*)]. \tag{6}$$

Since the impedance is only measured for positive frequencies; H_l can be approximated as

$$H_l(j\omega) \simeq r_l/(j\omega - b_l) = |r_l|e^{j\phi_l}/(j\omega - b_l), \tag{7}$$

where $|r_l|$ is the magnitude of the residue r_l, and ϕ_l is the phase of the residue r_l. Assuming r_l is unity, it can be shown that

$$(\mathrm{Re}[H_l] - (1/2\zeta_l\omega_l))^2 + (\mathrm{Im}[H_l])^2 = (1/2\zeta_l\omega_l)^2, \tag{8a}$$

where

$$\mathrm{Re}[H_l(j\omega)] = \zeta_l\omega_l/((\zeta_l\omega_l)^2 + (\omega - \omega_{dl})^2) \tag{8b}$$

and

$$\mathrm{Im}[H_l(j\omega)] = -(\omega - \omega_{dl})/((\zeta_l\omega_l)^2 + (\omega - \omega_{dl})^2). \tag{8c}$$

Equations (8) indicate that the frequency response curve for a single mode is a circle in the vector diagram. The complex residue simply expands the diameter of the circle and rotates the circle counterclockwise by an angle ϕ_l in the complex plane. By curve fitting a circle to a number of data points in

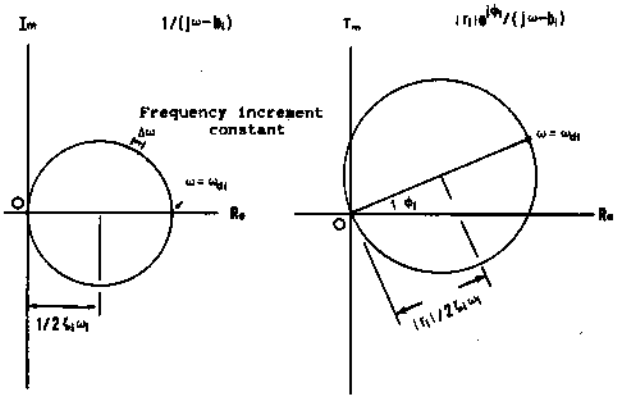

FIG. 6. Vector diagram method.

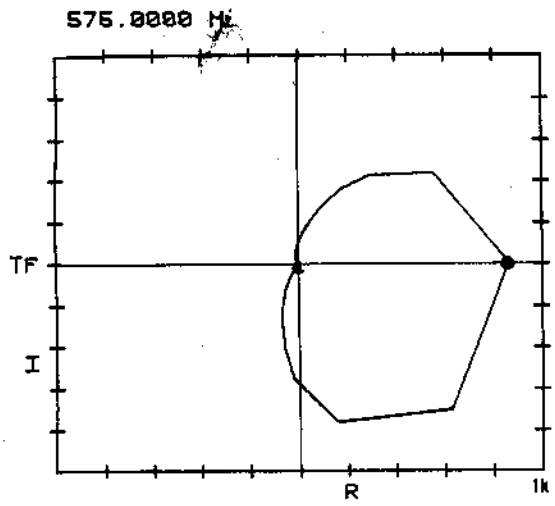

FIG. 7. Vector diagram of a typical acoustic transfer impedance near a resonant frequency and ● —location of resonance.

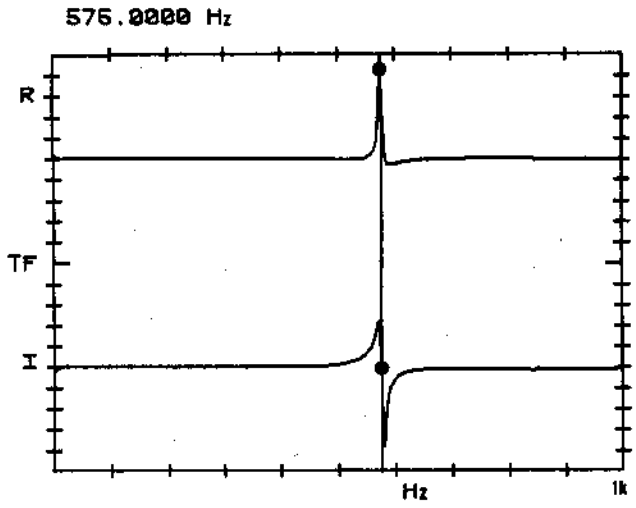

FIG. 8. Co-quad plot of a typical acoustic transfer impedance near a resonant frequency and ● —location of resonance.

the vicinity of each damped natural frequency, the pole and the residue for each mode can be extracted.

The natural frequency ω_i is identified as the frequency at a point on the circle where the spacing between points of equal frequency increment is a maximum. In other words, on the vector diagram $\Delta l/\delta\omega$ (where $\delta\omega$ = small variation in ω, Δl = arc length on vector diagram between and $\omega + \delta\omega$) is a maximum at a point where resonance occurs. Modal damping ratio ζ_i is given by $\zeta_i = d/2\omega_i$, where d is the half-power point bandwidth. The magnitude of the residue $|r_i|$ is equal to (circle diameter) $(\zeta_i\omega_i)$, and the phase of the residue is determined by measuring the angle between the positive real axis and the damped natural frequency diameter. Figures 7 and 8 show a typical vector diagram and the corresponding co-quad plot of a transfer impedance for a cylindrical cavity near the first resonance frequency. Modal parameters can easily be identified from either plot.

V. RESULTS AND DISCUSSION

Two example cases are discussed here. Example case I is a cylindrical cavity whose theoretical eigensolutions are well-known. Example case II is an annularlike cavity whose theoretical solutions are now known and therefore experimental results will be compared with those given by a finite element model of the cavity.

A. Example case I: A cylindrical cavity

For a cylindrical cavity, with both ends closed and of radius R and length L, containing a medium with speed of sound c, theoretical solutions for natural frequencies $f(i,m,n)$ and pressure mode shapes $\psi(i,m,n)$ are given by the following in cylindrical coordinates (r,θ,z) as[13]:

$$f(i,m,n) = c(k_z^2(i) + k_r^2(m,n))^{1/2}/2\pi, \tag{9a}$$

$$\psi(i,m,n) = \cos(k_z z)\begin{Bmatrix}\sin(k_\theta\theta)\\ \cos(k_\theta\theta)\end{Bmatrix} J_m(k_r r);$$

$$i,m,n = 0,1,2,..., \tag{9b}$$

where i,m,n are modal indices in longitudinal (z), circumferential (θ), and radial (r) directions, respectively, $k_r(m,n)$ is the

TABLE I. Natural frequencies and damping ratios for a cylindrical cavity (case I).

Mode number k	Modal indices (i,m,n)	Natural frequency $f(i,m,n) = \omega_k/2\pi$ Theory, Hz (a)	Experiment, Hz (b)	%Error $((b-a)/a)\times 100\%$	Experimental damping ratio ζ_k
1	(1,0,0)	557	575	−0.35	0.013
2	(0,1,0)	848	845	−0.35	0.009
3	(1,1,0)	1025	1020	−0.49	0.007
4	(2,0,0)	1154	1150	−0.35	0.006
5	(0,2,0)	1406	1395	−0.78	0.004
6	(2,1,0)	1432	1425	−0.49	0.004
7	(1,2,0)	1520	1510	−0.66	0.007
8	(3,0,0)	1731	1730	−0.06	0.006
9	(0,0,1)	1764	1765	−0.05	0.006
10	(2,2,0)	1819	1805	−0.77	0.005
11	(1,0,1)	1856	1845	−0.59	0.004
12	(3,1,0)	1927	1925	−0.10	0.010
13	(0,3,0)	1934	1930	−0.21	0.004

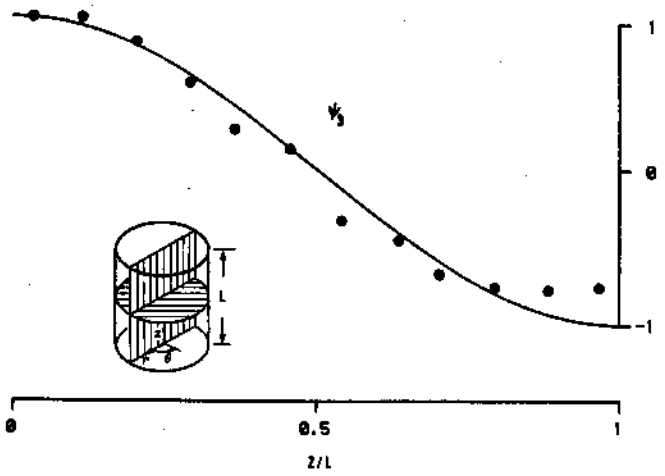

FIG. 9. Pressure mode ψ_3 along $r = R$, $\theta = 90°$, $z = 0 - L$; — theory, ● experiment.

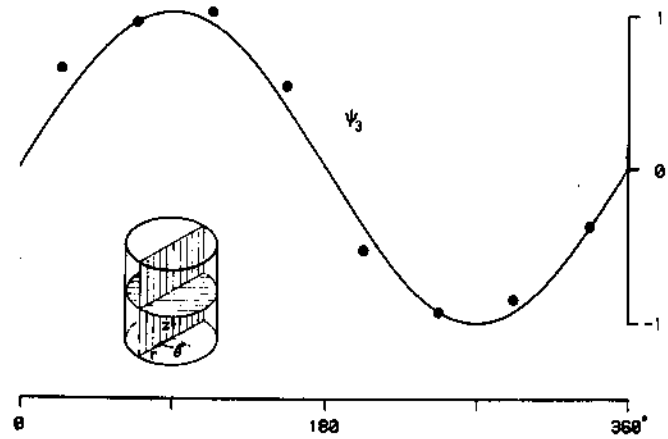

FIG. 10. Pressure mode ψ_3 along $r = R$, $z/L = 0.88$, $\theta = 0 - 360°$; — theory, ● experiment.

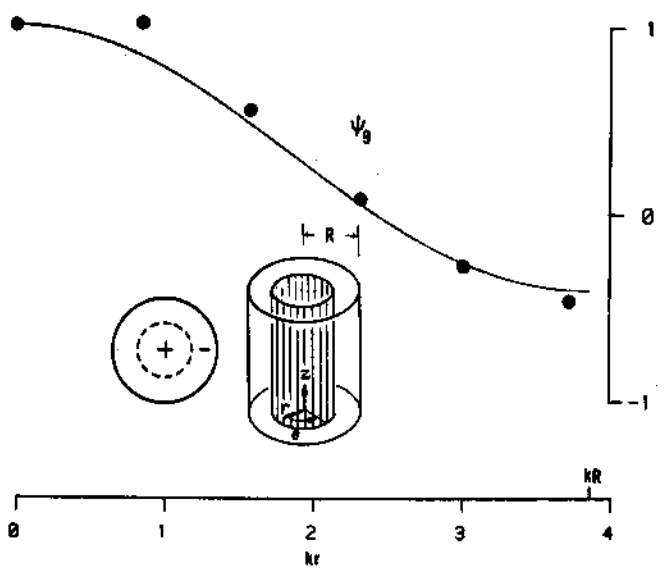

FIG. 11. Pressure mode ψ_9 along $z = L$, $\theta = 0°$, $r = 0 - R$; — theory, ● experiment.

radial wavenumber given by $J'_m(k_r R) = 0$, J_m is the Bessel function of the first kind of order m, $k_\theta = m$ is the circumferential wavenumber, and $k_z = \pi/L$ is the axial wavenumber. Since a boundary condition along θ does not exist, we get a set of orthogonal modes, as given by Eq. (9b), for index m. However in the experiment the location of the finite acoustic source fixes the circumferential mode, we can describe the mode shape only by $\sin m\theta$ where the origin of θ is maintained the same for the complete database. The experimental model constructed for testing purposes has a radius R of 119.1 mm and a length L of 298.5 mm. The boundary walls are nearly hard since the extracted modal damping ratios are less than 0.013 for all modes of interest as shown in Table I. The natural frequencies extracted from the transfer function data for air medium are compared with the exact solution (without damping) in Table I. Excellent agreement between theory and experiment is evident since the deviations from theoretical values are generally less than 1% of the theoretical values. Pressure mode shapes extracted experimentally are compared with the theoretical distributions in Figs. 9–11 for the third mode (1, 1, 0) and the ninth mode (0, 0, 1). These mode shapes are normalized such that both theoretical and experimental modes have the same maximum amplitude at the reference antinode. Again, excellent agreement between theory and experiment is evident.

B. Example case II: An annularlike cavity

Now we will consider a three-dimensional cavity whose theoretical solution is not known; it is bounded outside by a closed cylinder of radius $r_0 = 119.1$ mm and length $l_0 = 298.5$ mm and inside by a concentric cylindrical insert of radius $r_i = 90.5$ mm and length $l_i = 228.6$ mm. All walls are acoustically hard. The experimental model has nearly hard walls as extracted modal damping ratios are found to be less than 0.02 for all modes of interest (see Table II). The finite element model has 64 elements (8×8) for the "annular part" and eight elements (4×2) for the "cylindrical part" as shown in Fig. 12. The mesh size is chosen based such that the second mode shapes in θ and z directions and the first mode shape in the r direction can be described adequately. Only half of the cavity was modeled because of the symmetry.[14] The boundary conditions are that the derivatives of the acoustic pressure with respect to the boundary normals are zeros. More details of the finite element modeling aspects can be found in Refs. 14 and 15.

Table II shows the comparison of natural frequencies obtained from the experiment and the finite element model. Excellent correlation (1%–8% differences) is found here with deviations being larger for higher modes since the mesh size of the finite element model can no longer describe these modes adequately. Figure 13 shows typical acoustic pressure modes extracted experimentally and as displayed on a terminal capable of animations. The "wire frame" figure for each mode displays the variation of the acoustic pressure in θ direction (top view) and z direction (front view); the shaded planes indicate the nodal surfaces corresponding to each mode. Comparisons of the seventh mode (1,2,0) for experiment and finite-element model are shown in Figs. 14 and 15; the agreement again is also very good.

TABLE II. Natural frequencies and damping ratios for an annularlike cavity (case II).

Mode number k	Modal indices (i,m,n)	Natural frequency $f(i,m,n)=\omega_k/2\pi$ Experiment, Hz (a)	Finite element method, Hz (b)	% Difference $((b-a)/a)\times 100\%$	Experimental Damping ratio ζ_k
1	(1,0,0)	482	487	1	0.02
2	(0,1,0)	584	400	2.7	0.013
3	(1,1,0)	877	903	3	0.009
4	(2,0,0)	1067	1124	5	0.009
5	(0,2,0)	1130	1143	1.2	0.009
6	(2,1,0)	1258	1347	7	0.010
7	(1,2,0)	1326	1432	8	0.005

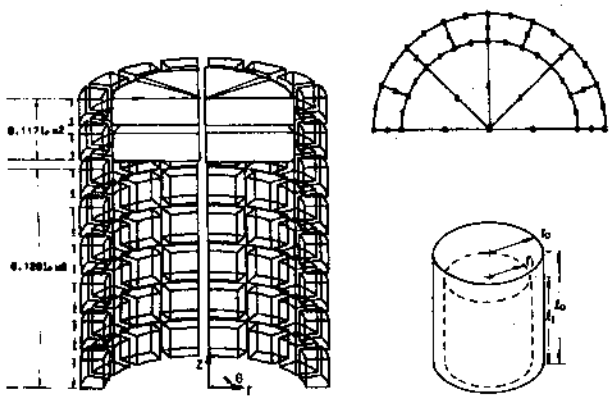

FIG. 12. Example case II: annularlike cavity and its finite element model.

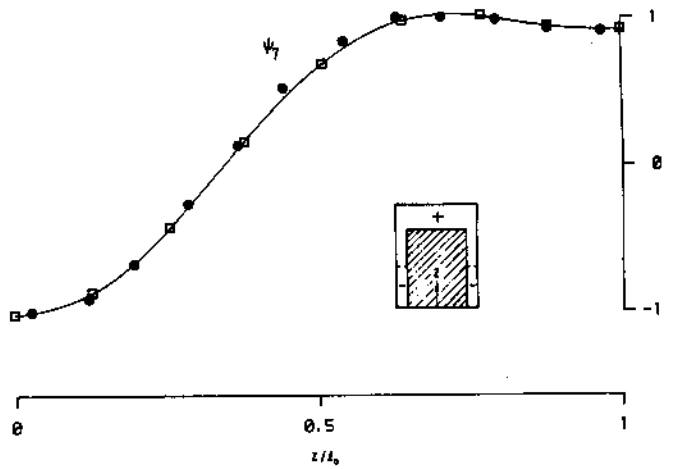

FIG. 14. Pressure mode ψ_7 along $r=r_0$, $\theta=0°$, $z=0-L$; ⊟ FEM, ● experiment.

VI. CONCLUDING REMARKS

In this paper, an experimental modal analysis technique for three-dimensional acoustic cavities has been proposed. The technique has been applied to a cylindrical cavity whose theoretical solution is known, and to an annularlike cavity which has no closed form solution. The experimental results obtained for the cylindrical cavity have been compared with the theoretical results, and they were found to be in excellent agreement. The application to the annularlike cavity also has been very successful since the experimental results closely match the results obtained from a finite element model.

The examples presented here have been limited to cavities with nearly hard walls; consequently, modes have been measured to be almost real. However, an acoustic cavity with nonproportional damping where complex modes exist, can also be modeled with ease since the formulation proposed here is based on complex numbers. Using multi-degree-of-freedom curve fitting techniques, heavily damped modes could also be extracted accurately.

It should be pointed out that in our example cases the pressure responses have been measured only on the bound-

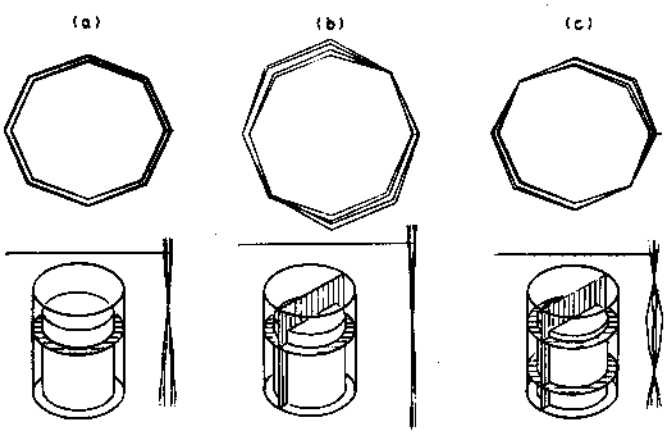

FIG. 13. Typical pressure modes extracted from experiment for example case II: (a) mode (1,0,0). (b) Mode (1,1,0). (c) Mode (2,1,0).

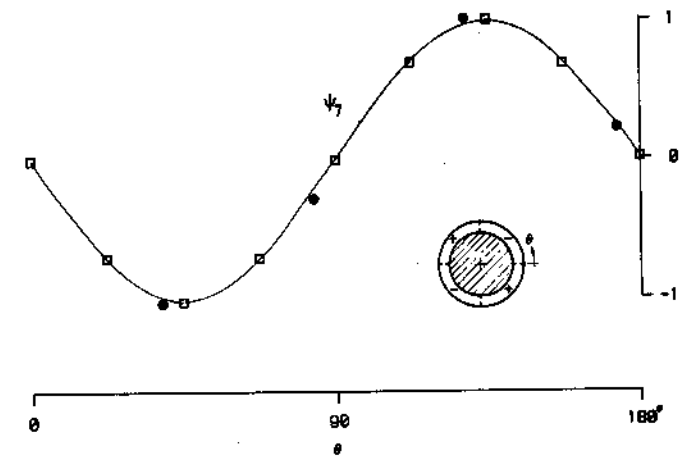

FIG. 15. Pressure mode ψ_7 along $r=r_0$, $z/l_0=0.88$, $\theta=0-180°$; ⊟ FEM, ● experiment.

ary, which enables us to define modes of interest completely. There should be no difficulty in measuring pressure responses within the cavity by inserting slender microphone probes.

Overall we believe that this paper makes a significant contribution to the field of experimental acoustics as it advances Nieter and Singh's method substantially. This paper also offers an alternative to the finite element method when irregular geometry and/or complicated boundary conditions are encountered. Further experimental work in this general area should be focused on the following complicating factors; presence of mean fluid flow, nonproportional damping, finite acoustic amplitudes, etc.

ACKNOWLEDGMENTS

The work reported here was sponsored by the Carrier Corporation, Syracuse, New York. The authors thank T. Katra, J. Crofoot, and P. Baade for their assistance.

[1]P. M. Morse and K. U. Ingard, *Theoretical Acoustics* (McGraw-Hill, New York, 1968).

[2]M. Petyt, G. H. Koopmenn, and K. J. Pinnington, "The Acoustic Modes of a Rectangular Cavity Containing a Rigid, Incomplete Partition," J. Sound Vib. **53** (1), 71–82 (1977).

[3]M. K. Au-Yang, "Pump-Induced Acoustic Pressure Distribution in an Annular Cavity Bounded by Rigid Walls," J. Sound Vib. **62** (4), 577–591 (1979).

[4]A. L. Klosterman, "On the Experimental Determination and Use of Modal Representation of Dynamic Characteristics," Ph.D. dissertation, University of Cincinnati (1971).

[5]M. Richardson, "Modal Analysis Using Digital Test Systems," Seminar on Understanding Digital Control and Analysis in Vibration Test Systems, Shock and Vibration Information Center, Washington, DC, Vol. 2, 43–64 (1975).

[6]M. Richardson and J. Kriskern, "Identifying Modes of Large Structures from Multiple Input and Response Measurements," SAE pap. 760875 (1976).

[7]H. G. Godyer, "Methods and Application of Structural Modelling from Measured Structural Frequency Response Data," J. Sound Vib. **68** (2), 209–230 (1980).

[8]M. Rades, "Analysis Techniques of Experimental Frequency Response Data," Shock Vib. Dig. **11** (2), 11 (1979).

[9]R. Singh, "Acoustic Impedance Measurement Methods," Shock Vib. Dig. **14** (2), 3–9 (1982).

[10]J. J. Nieter and R. Singh, "Acoustic Modal Analysis Experimental," J. Acoust. Soc. Am. **72**, 319–326 (1982).

[11]R. Singh and M. Schary, "Acoustic Impedance Measurement Using Sine Sweep Excitation and Known Volume Velocity Technique," 995–1005 (1978).

[12]O. C. Zienkiewicz, *The Finite Element Method* (McGraw-Hill, New York, 1977).

[13]R. D. Blevins, *Formulas for Natural Frequency and Mode Shape* (Van Nostrand, New York, 1979).

[14]C. H. Kung, "Finite Element and Experimental Modeling of Three-Dimensional Annular-Like Acoustic Cavities Using the Normal Mode Approach," Ph.D. dissertation, The Ohio State University (1984).

[15]C. H. Kung and R. Singh, "Finite Element Modeling of Annular-like Cavities," to be presented at the 1984 Winter Annular Meeting of ASME; also accepted for publication in J. Vib., Acoust. Stress Reliability Design (ASME Trans.).